Z' mediated right-handed neutrinos from meson decays at the FASER

Jiale Li,[1] Wei Liu,[2,*] and Hao Sun[1,†]

[1]*Institute of Theoretical Physics, School of Physics, Dalian University of Technology, No. 2 Linggong Road, Dalian, Liaoning 116024, People's Republic of China*

[2]*Department of Applied Physics and MIIT Key Laboratory of Semiconductor Microstructure and Quantum Sensing, Nanjing University of Science and Technology, Nanjing 210094, China*

(Received 19 September 2023; accepted 1 February 2024; published 27 February 2024)

We investigate the pair production of right-handed neutrinos mediated by a Z' mainly from the meson decays at the FASER detector of the HL-LHC. The Z' can be the additional gauge boson in either the $U(1)_{B-L}$ or sterile ν-specific $U(1)_s$ model. Taking the gauge coupling or the kinetic mixing at the current limits, we analyze the sensitivity to the masses of the heavy neutrinos, M_N, and active-sterile mixing, $|V_{lN}|^2$, of FASER2. In a background-free scenario, for the $U(1)_{B-L}$ case, FASER2 is able to probe $|V_{lN}|^2 \approx 10^{-8}$ when $M_N \sim 0.3$ GeV, which is comparable to the current limits from the beam dump experiments. When comes to the $U(1)_s$ model, FASER2 can probe $|V_{lN}|^2 \approx 10^{-10}$, which is better than the current limits for at least one magnitude, in all three flavors. A proposed long-lived particle detector, FACET, is also studied, but no significant difference from FASER2 is derived.

DOI: 10.1103/PhysRevD.109.035022

I. INTRODUCTION

In the Standard Model (SM), neutrinos are predicted to be massless fermions. Nevertheless, tiny neutrino masses have been observed at neutrino oscillation experiments, pointing the existence of the physics beyond the SM [1,2]. To explain the mass of neutrino, the seesaw mechanisms were proposed, arguing that neutrino masses are produced by adding massive right-handed neutrinos (RHNs). In this way the Dirac and Majorana mass terms can be added, thus giving the light neutrino mass with natural Yukawa couplings.

The RHNs can mix to the active neutrinos via the mixing V_{lN}, and $m_\nu \sim {V_{lN}}^2 M_N$ according to the canonical type-I seesaw. Various theoretical and experimental studies have been done to search for RHNs [3–28]. From the existing experiments, including the ones from beam-dump and collider experiments, the current limits set $|V_{lN}|^2 \lesssim 10^{-8}$ for RHNs with masses of $\mathcal{O}(0.1)$ GeV [29]. In such case, the RHNs can be long-lived particles (LLPs), and hence can lead to unique signatures at the LHC, with final states produced meters away from the interaction points.

Several detectors at the LHC aiming to detect such LLPs, have been proposed, including FASER [30], FACET [31], MATHUSLA [32], MoEDAL-MAPP [33], CODEX-b [34], ANUBIS [35], etc. Among them, FASER and MoEDAL-MAPP are already operating and others are still in discussions. Investigation of how to use these detectors to probe the RHNs have already been done in the existing literature. For example, Ref. [36] studied the RHNs from meson decays at the FASER.

On the other hand, the seesaw mechanism can be incorporated into ultraviolet-complete models, with the $U(1)_{B-L}$ model being one of the simplest [37,38]. In such a model, a $B-L$ gauge boson, Z' is also introduced which can be coupled to the quarks, and hence mesons. Therefore, Z' can be probed from meson decays at the FASER, as done in Ref. [39]. As the Z' can decay into RHNs, so the $Z' \to NN$ processes have also been used to probe the RHNs at the LHC [21], as well as the FCC-hh [22]. Similar processes have also been considered in Refs. [40,41] at FASER for the sterile ν-specific $U(1)_s$ model, where the Z' is dominantly produced from bremsstrahlung process and scatterings off electrons. Since it has not been discussed in detail, it becomes interesting to investigate the possibility of using Z'-mediated RHNs from meson decays at the FASER for both the $U(1)_{B-L}$ and $U(1)_s$ models. In this situation, the rates of the RHN events should also depend on the coupling or the kinetic mixings, in addition to the M_N and $|V_{lN}|^2$.

In this work, we study the sensitivity of FASER to the RHNs in the parameter space of $(M_N, |V_{lN}|^2)$, via the processes, meson $\to Z' \to NN$ (including bremsstrahlung), at the high-luminosity runs of the LHC (HL-LHC), with

*corresponding author: wei.liu@njust.edu.cn
†corresponding author: haosun@dlut.edu.cn

$\mathcal{L} = 3000\ \text{fb}^{-1}$. In addition to the original $U(1)_{B-L}$ model, we also consider the case where the Z' is assumed to strongly interact with the RHNs, with $g_X = 1$, while feebly to the SM particles, so-called the sterile ν-specific $U(1)_s$ model. These processes are sensitive to the RHNs with $0.1\ \text{GeV} < M_N < 10\ \text{GeV}$. We have taken the masses of the Z' from 0.5–2.5 GeV or fixed $M_{Z'} = 3M_N$. The gauge couplings or the kinetic mixings are taken at its maximal allowed value. The sensitivity of FACET is also studied, with no significant difference to the FASER obtained.

The paper is organized as follows, in Sec. II, we briefly review the $U(1)_{B-L}$ as well as the $U(1)_s$ model. Next, we introduce the analyses of the signal events in Sec. III. In Sec. IV, we show the resulting FASER sensitivity for different flavors. Finally, we conclude in Sec. V.

II. MODEL

A. $U(1)_{B-L}$ model

The relevant Lagrangian for the Z' and RHNs in the $U(1)_{B-L}$ model is [42,43]

$$\mathcal{L} \supset y_N \bar{N}^c N \chi + y_D \bar{L} N \tilde{H} + g_{B-L} Y_{B-L} \bar{f} \gamma^\mu Z' f + g_{B-L} Y_{B-L} \bar{N} \gamma^\mu Z' N + \text{H.c.}, \tag{1}$$

with $\tilde{H} = i\sigma^2 H^*$, N are the RHNs, f is the SM fermions plus the RHNs, Y_{B-L} is the $U(1)_{B-L}$ quantum number and χ is the $B-L$ scalar.

After the spontaneous symmetry breaking of the $U(1)_{B-L}$ and the SM, the completed mass matrix of the N can be written as

$$\mathcal{M} = \begin{pmatrix} 0 & m_D \\ m_D & m_R \end{pmatrix}, \tag{2}$$

where

$$m_D = \frac{y^D}{\sqrt{2}} v, \qquad m_R = \sqrt{2} y^N x, \tag{3}$$

with x being the vacuum expectation value of the $B-L$ scalar.

In the seesaw limit where the masses of RHNs are much larger than the active neutrinos, i.e., $m_R \gg m_D$, their masses are approximately,

$$m_\nu \sim -m_D m_R^{-1} m_D^T, \qquad M_N \sim m_R, \tag{4}$$

which recovers the type-I seesaw.

The flavor and mass eigenstates of the light and heavy neutrinos are connected as

$$\begin{pmatrix} \nu_L \\ \nu_R \end{pmatrix} = \begin{pmatrix} V_{LL} & V_{LR} \\ V_{RL} & V_{RR} \end{pmatrix} \begin{pmatrix} \nu \\ N \end{pmatrix}, \tag{5}$$

where $V_{LL} \approx U_{\text{PMNS}}$ and $V_{RR} \sim 1$, so the states of the heavy neutrinos and RHNs are roughly the same. The active-sterile mixings $V_{LR} = V_{LR} \equiv V_{lN}$, control the interaction of the RHNs to the active neutrinos.

Now we move to the Z', which has been searched for in various experiments. In our parameter space of interest, with $M_{Z'} \sim \mathcal{O}(\text{GeV})$, the current limits show $g_{B-L} \lesssim 2 \times 10^{-4}$ [44] as we take the maximal allowed value to get an optimistic sensitivity.

For our main processes, meson $\to Z' \to NN$, the Feynman diagram is shown in Fig. 1. The dominant mesons are the neutral pseudocscalar, π^0 and η at the LHC, whereas the direct production of the Z' via bremsstrahlung is also considered. Since the RHN pairs are produced from the on shell decays of the Z', the cross section of the signal processes can be estimated as

$$\sigma_S = \sigma(\pi^0/\eta \to Z'\gamma) \times \text{BR}(Z' \to NN), \tag{6}$$

where [39]

$$\sigma(\pi^0/\eta \to Z'\gamma) = \sigma_M \times 2(g_{B-L}/e)^2 \times \text{BR}(\pi^0/\eta \to \gamma\gamma) \times (1 - M_{Z'}^2/m_{\pi^0/\eta}^2)^3, \tag{7}$$

where σ_M is the cross section of mesons(π^0, η) and $\text{BR}(Z' \to NN) \approx 10\%$ for each flavors of N as taken from Ref. [21]. Z' can also be produced via proton bremsstrahlung, and the cross section of the signal processes can be estimated as

$$\sigma_S = \sigma_B \times \text{BR}(Z' \to NN), \tag{8}$$

where σ_B is the cross section of Z' produced from bremsstrahlung. Since we focus on the light RHNs, the production from Drell-Yan processes is negligible.

The N subsequently decay dominantly via three-body decays by an off shell W/Z boson. The expression of the decay width for N dominantly coupled to l_1 flavor reads [45]

$$\Gamma(N \to l_1^- l_2^+ \nu_{l_2}) = |V_{l_1 N}|^2 \frac{G_F^2}{192\pi^3} M_N^5 I_1(y_{l_1}, y_{\nu_{l_2}}, y_{l_2}) \times (1 - \delta_{l_1 l_2}), \tag{9}$$

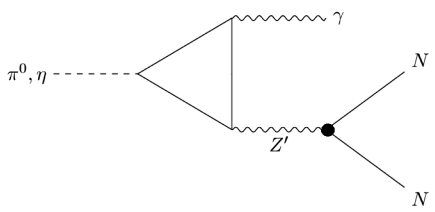

FIG. 1. The Feynman diagram of the process meson $\to Z' \to NN$.

$$\Gamma(N \to \nu_{l_1} l_2^- l_2^+) = |V_{l_1 N}|^2 \frac{G_F^2}{96\pi^3} M_N^5 [(g_L^l g_R^l + \delta_{l_1 l_2} g_R^l) \times I_2(y_{\nu_{l_1}}, y_{l_2}, y_{l_2}) \tag{10}$$

$$+ ((g_L^l)^2 + (g_R^l)^2 + \delta_{l_1 l_2}(1 + 2g_L^l)) \times I_1(y_{\nu_{l_1}}, y_{l_2}, y_{l_2})], \tag{11}$$

$$\sum_{l_2 = e,\mu,\tau} \Gamma(N \to \nu_{l_1} \nu_{l_2} \bar{\nu}_{l_2}) = |V_{l_1 N}|^2 \frac{G_F^2}{96\pi^3} M_N^5, \tag{12}$$

$$\Gamma(N \to l_1^- P^+) = |V_{l_1 N}|^2 \frac{G_F^2}{16\pi} M_N^3 f_P^2 |V_P|^2 F_P(y_{l_1}, y_P), \tag{13}$$

$$\Gamma(N \to \nu_{l_1} P^0) = |V_{l_1 N}|^2 \frac{G_F^2}{64\pi} M_N^3 f_P^2 (1 - y_P^2)^2, \tag{14}$$

$$\Gamma(N \to l_1^- V^+) = |V_{l_1 N}|^2 \frac{G_F^2}{16\pi} M_N^3 f_V^2 |V_V|^2 F_V(y_{l_1}, y_V), \tag{15}$$

$$\Gamma(N \to \nu_{l_1} V^0) = |V_{l_1 N}|^2 \frac{G_F^2}{2\pi} M_N^3 f_V^2 \kappa_V^2 (1 - y_V^2)^2 (1 + 2y_V^2), \tag{16}$$

where the kinematic functions $I_{(1,2)}(x, y, z)$, $F_{P,V}(x, y)$, leptonic couplings $g^l_{(L,R)}$, and meson decay constant $f_{(P,V)}$ are given in Ref. [45], and $y_i \equiv m_i / M_N$, with $m_i = m_P, m_V, m_l, m_q$.

B. Sterile ν-specific $U(1)_s$ model

The relevant Lagrangian for the Z' and Dirac RHNs in the $U(1)_s$ model is [41,42]

$$\mathcal{L} \supset y_s \bar{N} v_s \phi^\dagger + y_D \bar{L} N \tilde{H} + g_X \epsilon \cos\theta_W Q \bar{f} \gamma^\mu Z' f + g_X \bar{N} \gamma^\mu Z' N + \text{H.c.}, \tag{17}$$

with $\tilde{H} = i\sigma^2 H^*$, N the RHNs, and f being the SM fermions. Y is the quantum number and χ is SM singlet scalar field.

The cross section of the signal processes now depend on the mixing ϵ,

$$\sigma(\pi^0/\eta \to Z'\gamma) = \sigma_M \times 2\epsilon^2 \times \text{BR}(\pi^0/\eta \to \gamma\gamma) \times (1 - M_{Z'}^2/m_{\pi^0/\eta}^2)^3, \tag{18}$$

and the current limit points $\epsilon \lesssim 6 \times 10^{-4}$ in our parameter space [39].

In this model, we can have $g_X \sim 1 \gg \epsilon$; therefore, the $\text{BR}(Z' \to NN) \approx 100\%$, if only one flavor of N is coupled to the Z'. Instead of decaying via an off shell W/Z boson at the $U(1)_{B-L}$ model, now the major decay channel is via an off shell Z'. Hence, the decay length of N in this model can be much smaller than the $U(1)_{B-L}$ model for fixed $|V_{lN}|^2$. The decay channels via an off shell Z' can be expressed as

$$\Gamma(N \to \nu_{l_1} l_2^- l_2^+) = |V_{l_1 N}|^2 \frac{G_X^2 \epsilon^2}{48\pi^3} M_N^5 [I_2(y_{\nu_{l_1}}, y_{l_2}, y_{l_2}) + 2I_1(y_{\nu_{l_1}}, y_{l_2}, y_{l_2})], \tag{19}$$

$$\sum_{l_2 = e,\mu,\tau} \Gamma(N \to \nu_{l_1} \nu_{l_2} \bar{\nu}_{l_2}) = |V_{l_1 N}|^2 \frac{G_X^2 \epsilon^2}{48\pi^3} M_N^5, \tag{20}$$

$$\Gamma(N \to \nu_{l_1} P^0) = |V_{l_1 N}|^2 \frac{G_X^2 \epsilon^2}{32\pi} M_N^3 f_P^2 (1 - y_P^2)^2, \tag{21}$$

$$\Gamma(N \to \nu_{l_1} V^0) = |V_{l_1 N}|^2 \frac{G_X^2 \epsilon^2}{\pi} M_N^3 f_V^2 \kappa_V^2 (1 - y_V^2)^2 (1 + 2y_V^2), \tag{22}$$

where $G_X = g_X^2/(4\sqrt{2} M_{Z'}^2)$.

In Fig. 2 (left), we show the decay length of N for the $U(1)_{B-L}$ and the $U(1)_s$ model, respectively, where we fix $\epsilon = 6 \times 10^{-4}$ at the current limit, $g_X = 1$ and $|V_{lN}|^2 = 10^{-7}$. For the $U(1)_{B-L}$ model, in principle, the RHNs can also decay via an off shell Z'. Nevertheless, as we take $g_{B-L} \ll e$, the decay width is negligible compared to the weak decays [46]. Therefore, the decay width is only dependent on $|V_{lN}|^2$. For the $U(1)_s$ model, we take $g_X = 1$,

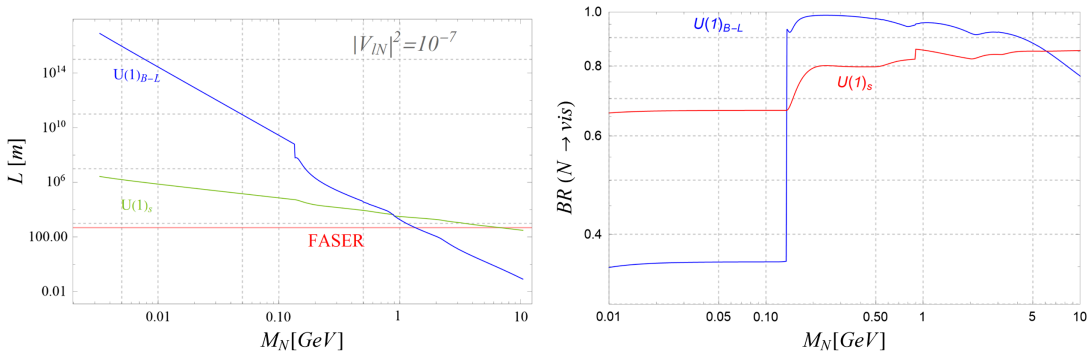

FIG. 2. Left: The decay length of the N for the $U(1)_{B-L}$ and $U(1)_s$ model. Right: The branching ratio of the N decays into visible final states for the two models. We fix $|V_{lN}|^2 = 10^{-7}$, where $l = e, \mu, \tau$, and N only couple to one flavor each, and $\epsilon = 6 \times 10^{-4}$, $g_X = 1$.

and $M_{Z'} \ll M_Z$, hence N decays via an off shell Z', and the decay width is dependent on both $|V_{lN}|^2$ as well as ϵ and g_X. When $M_N \lesssim 1$ GeV, $L(N)$ in the $U(1)_{B-L}$ is larger than the $U(1)_s$ case, while it becomes the opposite when $M_N \gtrsim 1$ GeV.

The branching ratio of the N decays into visible final states for the $U(1)_{B-L}$ and $U(1)_s$ models is shown in Fig. 2 (right). This is relevant to estimate the potential signal yield, as the experiments are more likely to observe visible final states, other than the $\nu\nu\nu$ final states. In the figure, we find that, once the N is heavier than light hadrons, e.g., π and η, $\mathrm{BR}(N \to vis) \gtrsim 90\%$ for the $U(1)_{B-L}$ model and above 80% for the $U(1)_s$ model.

III. ANALYSES

Now we estimate the number of signal events at the FASER, which should be

$$N_S = \sigma(\pi^0/\eta \to Z'\gamma) \times \mathrm{BR}(Z' \to N\,N) \times BR^2(N \to vis) \times \mathcal{P} \times \mathcal{L}, \tag{23}$$

where the P is of possibility of N decay inside the FASER volume, which is a function of momentum of the N and θ (the angle of the momentum and the beam line).

$$\mathcal{P}(p,\theta) = (e^{-(L-\Delta)/d} - e^{-L/d})\Theta(R - \tan\theta L) \approx \frac{\Delta}{d} e^{-L/d}\Theta(R - \theta L), \tag{24}$$

where L is the distance of the FASER to the interaction point, Δ is the depth of the FASER volume, d is the lab decay length of the N, and R is the radius of the FASER. The lab decay length takes account the Lorentz boost factor, $d = c\tau\beta\gamma = c\tau \times p/M_N$.

Since p, θ of the N is a distribution, the number of signal events becomes

$$N_S = \mathcal{L} \int dp d\theta \frac{d\sigma}{dp d\theta} \times \mathcal{P}(p,\theta). \tag{25}$$

The FASER detector is going to be operated in two phases [30,47],

$$\textbf{FASER1}:\ L = 480\ \mathrm{m}, \Delta = 1.5\ \mathrm{m}, R = 10\ \mathrm{cm}, \mathcal{L} = 150\ \mathrm{fb}^{-1},$$
$$\textbf{FASER2}:\ L = 480\ \mathrm{m}, \Delta = 10\ \mathrm{m}, R = 1\ \mathrm{m}, \mathcal{L} = 3\ \mathrm{ab}^{-1}. \tag{26}$$

Since the volume of FASER1 is too small, in the following calculation, we focus on the FASER2 setup. There is also a trigger requirement on the RHNs, such that $p > 100$ GeV.

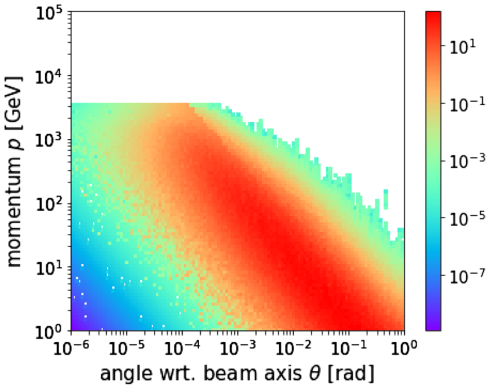

FIG. 3. The spectrum of the momentum, p and angle to the beam axis θ for the Z', with $M_{Z'} = 0.1$ GeV and $g_{B-L} = 2 \times 10^{-4}$, generated by using the FORESEE package [39].

We also consider the FACET detector [48], with

$$\textbf{FACET}:\ L = 101\ \mathrm{m}, \Delta = 11\ \mathrm{m}, R = 0.18 - 0.5\ \mathrm{m}, \mathcal{L} = 3\ \mathrm{ab}^{-1}. \tag{27}$$

In order to estimate the number of signal events via the aforementioned methods, we use the FORESEE PYTHON package in Ref. [39]. The kinematic distribution of various mesons in the one forward hemisphere have already been stored in the FORESEE package. Once we provide the formulas for the production of the Z' from mesons as well as bremsstrahlung, the package can output the differential spectra $[d\sigma(M \to Z')/dp_{Z'}d\cos\theta_{Z'}]$ of the Z', where $p_{Z'}$ is the 3-momentum and $\theta_{Z'}$ is the polar angle. The kinematic distribution of the Z' is shown in Fig. 3. As Z' decays into two identical N, $p_N \approx p_{Z'}/2$ and $\theta_N \approx \theta_{Z'}$, since $p_N \gg M_N$ in the forward direction. Therefore, the distribution of the p, θ for the N should be very similar to the ones for the Z'. From Fig. 3, we can see that, since Z' is mainly produced via the decays of mesons, therefore their transverse momentum $p_T \sim \Lambda_{\mathrm{QCD}}$, that is why most of the particles are distributed at the forward direction. For the FASER2 location where $\theta \sim 2 \times 10^{-3}$ and the trigger requirement is $p > 100$ GeV; there are still hundreds of events, and we use Eq. (25) to estimate the number of signal events at the FASER2.

IV. RESULTS AND DISCUSSIONS

In this section, we show the expected sensitivity of FASER2 to the right-handed neutrinos in the selected parameter space. We take 3000 fb^{-1} integrated luminosity for FASER2. Since the N can decay into pairs of visible particles, their vertex can be reconstructed at the FASER2. The detectors are shields from hundreds of meters from the IP of the LHC, so the background in this case is negligible; hence we only require $N_S > 3$ to define the sensitivity at 95% confidence level.

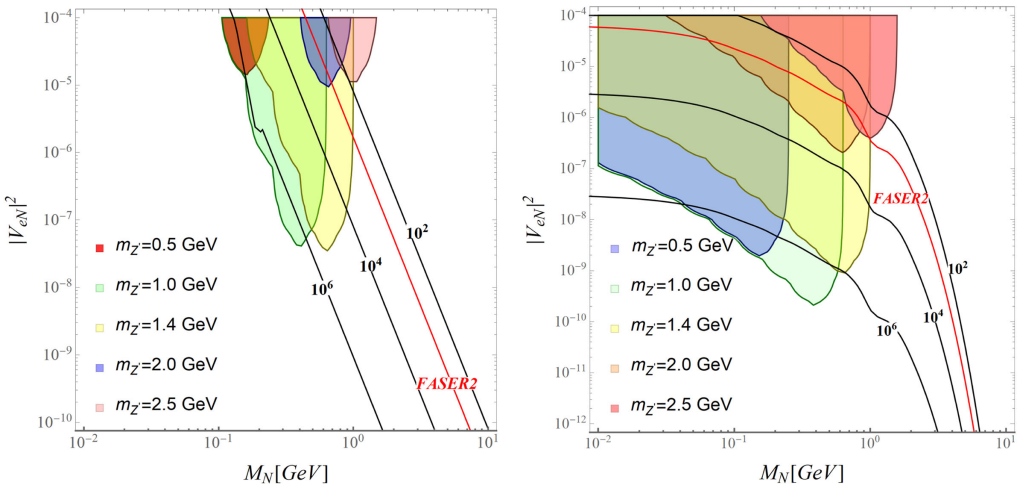

FIG. 4. Left: The sensitivity on the $(M_N, |V_{eN}|^2)$ plane of FASER2, for the $U(1)_{B-L}$ model. We fixed $M_{Z'} = 0.5$ GeV, 1.0 GeV, 1.4 GeV, 2.0 GeV, 2.5 GeV, as indicated by red, green, yellow, blue, and pink bands, respectively. The curves represent the fixed values of the proper decay length of N, $L(N) = 10^{2,4,6}$, and 480 meters which is the distance from the FASER2 to the LHC's IP are overlaid for comparison. The gauge coupling is fixed at $g_{B-L} = 2 \times 10^{-4}$. Right: The same but for the $U(1)_s$ model, and the kinetic mixing is fixed at $\epsilon = 6 \times 10^{-4}$.

Overall, the number of the signal events depends on four free parameters, $(M_N, |V_{lN}|^2, M_{Z'}, g_{B-L}/\epsilon)$. In order to probe the RHNs, i.e., to obtain sensitivity in the $(M_N, |V_{lN}|^2)$ plane, we need to fix the $M_{Z'}$ and g_{B-L}/ϵ. As mentioned in the text, we always fix the coupling or the mixing g_{B-L}/ϵ at the maximally allowed values by the current limits. For $M_{Z'}$, we begin with fixed values of 0.5 GeV, 1.0 GeV, 1.4 GeV, 2.0 GeV, and 5.0 GeV, and followed by fixed ratios of $M_{Z'} = 3M_N$.

In Fig. 4 we show the sensitivity on the $(M_N, |V_{eN}|^2)$ plane, for both the $U(1)_{B-L}$ (left) and $U(1)_s$ (right) models. The solid curves represent the fixed values of the proper decay length of N, $L(N) = 10^{2,4,6}$, and 480 meters which is the distance from the FASER2 to the LHC's IP are overlaid for comparison. Since the N is largely boosted at the forward direction, the lab decay length can even be much larger, e.g., by 10^3 times. For the $U(1)_{B-L}$ model, the best sensitivity is obtained as $|V_{eN}|^2 \sim 10^{-7}$ where $M_N \approx 0.3$ GeV when $M_{Z'} = 1(1.4)$ GeV. In such a scenario, the Z' is heavy enough to let the N have its decay length close to the FASER2's distance to the IP, and not so heavy so the Z' cannot be produced by meson decays and bremsstrahlung. When it comes to the $U(1)_s$ model, it benefits from the decay length of the N being much closer to the FASER2 for fixed $|V_{eN}|^2$ and larger decay branching ratio from Z', now we can get almost three times better sensitivity as we approach $|V_{eN}|^2 \sim 10^{-10}$, where $M_N \approx 0.5$ GeV when $M_{Z'} = 1$ GeV.

Now we move to the scenarios where we fix $M_{Z'} = 3M_N$. The results are shown in Figs. 5–7, where the results are compared with the current limits from different existing experiments for the RHNs to be dominated coupled to e, μ, and τ leptons, respectively. In our parameter space, for the electron flavor, the most powerful existing constraints come from the beam dump experiments NA62 [49] as well as T2K [50], mainly from the process $K \to lN$, $l = e, \mu$, and hence is sensitive to $M_N \approx m_K \approx 0.5$ GeV. Both of the detectors are put $\mathcal{O}(10^2)$ meters away from the beam, similar to the FASER. Other beam dump experiments, PIENU [51], BEBC [52], and PS191 [53] also searched for the RHNs, whereas their constraints are not competitive as the aforementioned ones. Nevertheless, the PS191 and PIENU searched the $\pi \to lN$, and BEBC searched the $\tau \to XXN$, thus can be sensitive to $M_N \lesssim 0.2$ GeV and $M_N \gtrsim 0.5$ GeV which is not probed by NA62 and T2K. In addition, the RHNs have also been searched via the direct production at electron-positron

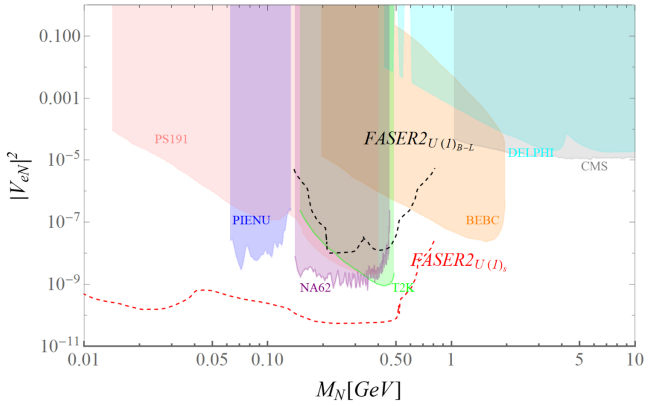

FIG. 5. The sensitivity on the $(M_N, |V_{lN}|^2)$ of the FASER2 for the $U(1)_{B-L}$ (dashed black) and $U(1)_s$ (dashed red) model, when $l = e$. Current limits from NA62 [49], T2K [50], PIENU [51], DELPHI [54], CMS [59], BEBC [52], and PS191 [53] are overlaid for comparison.

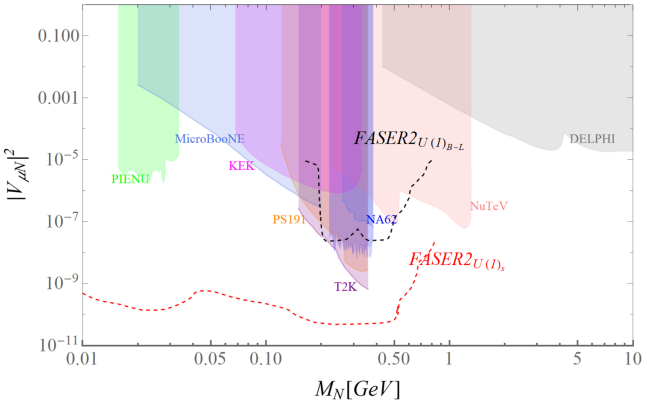

FIG. 6. The same as Fig. 5, but for $l = \mu$. Current limits from NA62 [49], T2K [50], PIENU [51], DELPHI [54], PS191 [53], KEK [55], NuTeV [56], and MicroBooNE [57] are overlaid for comparison.

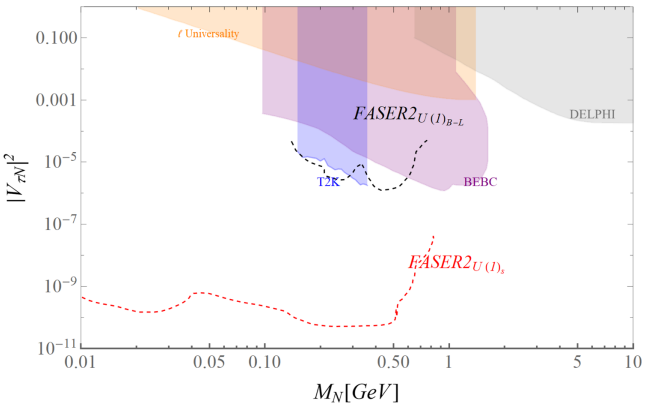

FIG. 7. The same as Fig. 5, but for $l = \tau$. Current limits from T2K [50], BEBC [52], DELPHI [54], and the lepton universality test [58].

colliders, $e^+e^- \to Z \to N\nu$ at the DELPHI experiment at the LEP [54]. When it comes to the muon flavor, the different masses of the muon and electron translate the constraints to the lower M_N. In addition, KEK [55], NuTeV [56], and MicroBooNE [57] also searched for RHNs with the muon flavor. For the tau flavor only a few experiments, including T2K, BEBC, DELPHI, as well as the lepton universality test [58] are available with much looser constraints, since the tau lepton is hard to detect.

Unlike the case for fixed $M_{Z'}$, now the kinematics threshold requiring Z' to decay into two Ns is spontaneously satisfied; hence, the reach to the mass of the Ns extends to wider regions. Despite the different reconstruction efficiencies for the leptons at the FASER2 which are yet unknown, the sensitivity from the FASER2 should not depend on the flavor of the RHNs. For the $U(1)_{B-L}$ model, the sensitivity of the FASER2 reaches the lowest $|V_{lN}|^2 \approx 10^{-8}$ when $M_N \sim 0.3$ GeV, so that the Z' is roughly resonantly produced by the decay of the η meson. The sensitivity of $|V_{lN}|^2$ becomes drastically worse to $|V_{lN}|^2 \approx 10^{-5}$ when we move to the lower and larger M_N, since either the decay length is too large or the production cross section is too small.

For the $U(1)_{B-L}$ model, comparing it to the existing experiments on the electron flavor of the RHN, FASER2 roughly has the same sensitivity to the ones from the NA62 and T2K. When we consider RHNs heavier than m_K, the sensitivity of the FASER2 exceeds the current best limits from the BEBC. The situation is similar on the muon flavor, only now current best limits for RHNs heavier than m_K is from the NuTeV and also has been exceeded by the FASER2 via Z' decays. When it comes to the τ flavor, since the decay channel $N \to \tau^- XX$ is forbidden in most of our parameter space of interest, the decay length of the N becomes much larger so the sensitivity can only reach larger V_{lN}^2, which is close to the current limits as well.

As mentioned, in the $U(1)_s$ model the FASER2 should have much better sensitivity on the active-sterile mixings $|V_{lN}|^2$. As indicated by the red dashed lines in Figs. 5–7, the FASER2 can now probe the mixing as low as $|V_{lN}|^2 \sim 10^{-10}$, which is roughly two magnitudes better than the ones in the $U(1)_{B-L}$ model. This is better than the current limits for all three flavors of the RHNs; now the FASER2 is sensitive to M_N as low as 0.01 GeV, as the decay length for such light N is no longer dependant on the mass of N, but is dependant on the kinetic mixing ϵ in this model. Hence, in this case, the FASER2 has shown positive potential to reveal the origin of the neutrino mass problem, i.e., probing the RHNs. However, for the existing beam dump experiments, in order to get the right sensitivity, recasting should be done to consider the different decay lengths of N in the appearance of the $U(1)_s$ Z'.

V. CONCLUSION

The seesaw mechanism as explained in the neutrino oscillation experiment, the important goal of the study of neutrino mass is to find the right-handed neutrino. According to the seesaw mechanism, $m_\nu \sim |V_{lN}|^2 M_N$ [21]; hence, at the current limits for sub-GeV RHNs, they can be regarded as long-lived particles. The goal of our work is to look for RHNs and to estimate the sensitivity of the far detector FASER2 to the RHNs.

In this work we explore the sensitivity of FASER2 detector to the RHNs in meson $\to Z' \to NN$ channel. Both the $U(1)_{B-L}$ and sterile ν-specific $U(1)_s$ models are considered. In the former model, the Z' couples to all the fermion with the same gauge coupling, which we fixed at $g_{B-L} = 2 \times 10^{-4}$. While for the latter one, the Z' coupling to the RHNs can be sufficiently higher than the ones for SM fermions, $g_X \sim 1 \gg \epsilon = 6 \times 10^{-4}$. Hence, in the $U(1)_s$ model, the Z' almost only decay into RHNs, and the decay of the RHNs is dominated by a off shell Z'. For similar couplings and $|V_{lN}|^2$, the branching ratio of Z' to the RHNs is higher, and the decay length of the RHNs is

shorter and closer to the distance of the FASER2 to the IP if $M_N \lesssim 1$ GeV.

Two scenarios of the masses of Z' are discussed. In the first one, the masses are fixed at $M_{Z'} = 0.5$ GeV, 1.0 GeV, 1.4 GeV, 2.0 GeV, and 5.0 GeV. In the second one, the ratio between the masses of the RHNs and Z' is fixed at $M_{Z'} = 3M_N$. In both scenarios, we estimate the number of signal events after considering the decay length of the RHNs, and the geometrical information of the volume of the FASER2. With no background assumption, sensitivity to the $(M_N, |V_{lN}|^2)$ is obtained by asking $N_S > 3$.

We then compare our results with existing limits. Depending on the dominated couplings to the leptons of the RHNs, the current limits can be classified into three categories, the limits on $|V_{eN}|^2$, $|V_{\mu N}|^2$, and $|V_{\tau N}|^2$, respectively. Figure 5 gives the current constraints of electron mixing $|V_{eN}|^2$ which has been obtained experimentally. The experiments include PIENU [51], T2K [50], NA62 [49], BEBC [52], and DELPHI [54]. Figure 6 indicates the current limits on muon mixing $|V_{\mu N}|^2$ from NA62 [49], T2K [50], PIENU [51], DELPHI [54], PS191 [53], KEK [55], NuTeV [56], and MicroBooNE [57]. For the $U(1)_{B-L}$ model, as can be seen from the figures, our results reach $|V_{lN}|^2 \sim 10^{-8}$ and are comparable to the current limits overall. When the mass of N is less than 0.5 GeV (m_K), the results obtained by the current experiment are better. However, when the mass of N is more than 0.5 GeV (m_K) and less than about 0.6 GeV, our results are better than the current limits from BEBC/NuTeV. Figure 7 indicates the current limits on tau mixing $|V_{\tau N}|^2$ from T2K [50], BEBC [52], DELPHI [54], and the lepton universality test [58]. Now the current limits as well as the limits in this paper are rather poor since the decay into τ leptons final states is kinematically forbidden, and N are too long-lived to be detected by the FASER detector. When we move to the $U(1)_s$ model, the gain in larger N production from Z' decay, and closer decay length to the FASER2's volume lead to about two magnitudes better sensitivity on $|V_{lN}|^2$. For much lighter N with $M_N < 0.1$ GeV, since the decay length is controlled by the kinetic mixing ϵ instead of M_N, the sensitivity curves become roughly constant at $|V_{lN}|^2 \sim 10^{-10}$, where all the current limits can not reach.

We have shown that in certain scenarios FASER can yield better sensitivity than the current limits. However, the current limits are performed by sterile neutrinos only models, such that the RHNs are directly produced via the mixing from the weak decays, etc. Proper comparison between different detectors can be made if all the limits can be recast to the same model. However, even though the recast of the production can be feasible, the kinematic and detector efficiencies still require full Monte Carlo simulation, which we leave for future works.

We have obtained similar sensitivity from FACET, comparing to the FASER. Since the Z' is dominantly produced via light mesons π^0 and η, Z' and hence the RHNs are more likely to distribute in a forward direction where the FASER located. FACET's coverage in solid angle is several times larger although it placed closer to the transverse direction. Hence, in this study, the overall effects lead to similar sensitivity for both FACET and FASER. In a recent work, the processes where the RHNs are produced via the decays of D and B mesons are considered [48]. As the RHNs are now produced directly from massive mesons they are distributed closer to the transverse direction; hence the FACET turns out to be more sensitive.

ACKNOWLEDGMENTS

W. L. is supported by National Natural Science Foundation of China (Grant No. 12205153), and the 2021 Jiangsu Shuangchuang (Mass Innovation and Entrepreneurship) Talent Program (No. JSSCBS20210213). H. S. is supported by the National Natural Science Foundation of China (Grant No. 12075043). We thank Arindam Das for useful discussions.

[1] Y. Fukuda *et al.* (Super-Kamiokande Collaboration), Phys. Rev. Lett. **81**, 1562 (1998).
[2] Q. R. Ahmad *et al.* (SNO Collaboration), Phys. Rev. Lett. **89**, 011301 (2002).
[3] B. Batell, M. Pospelov, and B. Shuve, J. High Energy Phys. 08 (2016) 052.
[4] B. Bhattacherjee, S. Matsumoto, and R. Sengupta, Phys. Rev. D **106**, 095018 (2022).
[5] E. Accomando, L. Delle Rose, S. Moretti, E. Olaiya, and C. H. Shepherd-Themistocleous, J. High Energy Phys. 02 (2018) 109.
[6] A. Das, P. S. B. Dev, and N. Okada, Phys. Lett. B **799**, 135052 (2019).
[7] K. Cheung, K. Wang, and Z. S. Wang, J. High Energy Phys. 09 (2021) 026.
[8] C.-W. Chiang, G. Cottin, A. Das, and S. Mandal, J. High Energy Phys. 12 (2019) 070.
[9] P. Fileviez Pérez and A. D. Plascencia, Phys. Rev. D **102**, 015010 (2020).
[10] A. Das, N. Okada, S. Okada, and D. Raut, Phys. Lett. B **797**, 134849 (2019).
[11] A. Maiezza, M. Nemevšek, and F. Nesti, Phys. Rev. Lett. **115**, 081802 (2015).
[12] M. Nemevšek, F. Nesti, and J. C. Vasquez, J. High Energy Phys. 04 (2017) 114.

[13] J. D. Mason, J. High Energy Phys. 07 (2019) 089.
[14] E. Accomando, L. Delle Rose, S. Moretti, E. Olaiya, and C. H. Shepherd-Themistocleous, J. High Energy Phys. 04 (2017) 081.
[15] Y. Gao, M. Jin, and K. Wang, J. High Energy Phys. 02 (2020) 101.
[16] A. M. Gago, P. Hernández, J. Jones-Pérez, M. Losada, and A. Moreno Briceño, Eur. Phys. J. C **75**, 470 (2015).
[17] J. Jones-Pérez, J. Masias, and J. D. Ruiz-Álvarez, Eur. Phys. J. C **80**, 642 (2020).
[18] W. Liu, K.-P. Xie, and Z. Yi, Phys. Rev. D **105**, 095034 (2022).
[19] F. F. Deppisch, W. Liu, and M. Mitra, J. High Energy Phys. 08 (2018) 181.
[20] S. Amrith, J. M. Butterworth, F. F. Deppisch, W. Liu, A. Varma, and D. Yallup, J. High Energy Phys. 05 (2019) 154.
[21] F. Deppisch, S. Kulkarni, and W. Liu, Phys. Rev. D **100**, 035005 (2019).
[22] W. Liu, S. Kulkarni, and F. F. Deppisch, Phys. Rev. D **105**, 095043 (2022).
[23] W. Liu, J. Li, J. Li, and H. Sun, Phys. Rev. D **106**, 015019 (2022).
[24] Y. Zhang and W. Liu, Phys. Rev. D **107**, 095031 (2023).
[25] W. Liu and Y. Zhang, Eur. Phys. J. C **83**, 568 (2023).
[26] A. Das and N. Okada, Phys. Lett. B **774**, 32 (2017).
[27] B. Bhattacherjee, H. K. Dreiner, N. Ghosh, S. Matsumoto, R. Sengupta, and P. Solanki, arXiv:2306.11803.
[28] D. Barducci, W. Liu, A. Titov, Z. S. Wang, and Y. Zhang, Phys. Rev. D **108**, 115009 (2023).
[29] P. D. Bolton, F. F. Deppisch, and P. S. Bhupal Dev, J. High Energy Phys. 03 (2020) 170.
[30] J. L. Feng, I. Galon, F. Kling, and S. Trojanowski, Phys. Rev. D **97**, 035001 (2018).
[31] S. Cerci *et al.*, J. High Energy Phys. 06 (2022) 110.
[32] J. P. Chou, D. Curtin, and H. J. Lubatti, Phys. Lett. B **767**, 29 (2017).
[33] M. Frank, M. de Montigny, P.-P. A. Ouimet, J. Pinfold, A. Shaa, and M. Staelens, Phys. Lett. B **802**, 135204 (2020).
[34] V. V. Gligorov, S. Knapen, M. Papucci, and D. J. Robinson, Phys. Rev. D **97**, 015023 (2018).
[35] M. Hirsch and Z. S. Wang, Phys. Rev. D **101**, 055034 (2020).
[36] F. Kling and S. Trojanowski, Phys. Rev. D **97**, 095016 (2018).
[37] R. N. Mohapatra and R. E. Marshak, Phys. Rev. Lett. **44**, 1316 (1980); **44**, 1643(E) (1980).
[38] A. Davidson, Phys. Rev. D **20**, 776 (1979).
[39] F. Kling and S. Trojanowski, Phys. Rev. D **104**, 035012 (2021).
[40] K. Jodłowski and S. Trojanowski, J. High Energy Phys. 05 (2021) 191.
[41] Y. Jho, J. Kim, P. Ko, and S. C. Park, arXiv:2008.12598.
[42] E. Bertuzzo, S. Jana, P. A. N. Machado, and R. Zukanovich Funchal, Phys. Rev. Lett. **121**, 241801 (2018).
[43] P. Ballett, S. Pascoli, and M. Ross-Lonergan, Phys. Rev. D **99**, 071701 (2019).
[44] P. Ilten, Y. Soreq, M. Williams, and W. Xue, J. High Energy Phys. 06 (2018) 004.
[45] J. C. Helo, S. Kovalenko, and I. Schmidt, Nucl. Phys. **B853**, 80 (2011).
[46] A. Atre, T. Han, S. Pascoli, and B. Zhang, J. High Energy Phys. 05 (2009) 030.
[47] A. Ariga *et al.* (FASER Collaboration), Phys. Rev. D **99**, 095011 (2019).
[48] M. Ovchynnikov, V. Kryshtal, and K. Bondarenko, J. High Energy Phys. 02 (2023) 056.
[49] E. Cortina Gil *et al.* (NA62 Collaboration), Phys. Lett. B **807**, 135599 (2020).
[50] K. Abe *et al.* (T2K Collaboration), Phys. Rev. D **100**, 052006 (2019).
[51] A. Aguilar-Arevalo *et al.* (PIENU Collaboration), Phys. Rev. D **97**, 072012 (2018).
[52] R. Barouki, G. Marocco, and S. Sarkar, SciPost Phys. **13**, 118 (2022).
[53] G. Bernardi *et al.*, Phys. Lett. B **203**, 332 (1988).
[54] P. Abreu *et al.* (DELPHI Collaboration), Z. Phys. C **74**, 57 (1997); **75**, 580(E) (1997).
[55] A. V. Artamonov *et al.* (E949 Collaboration), Phys. Rev. D **91**, 052001 (2015); **91**, 059903(E) (2015).
[56] A. Vaitaitis *et al.* (NuTeV, E815 Collaboration), Phys. Rev. Lett. **83**, 4943 (1999).
[57] P. Abratenko *et al.* (MicroBooNE Collaboration), Phys. Rev. D **101**, 052001 (2020).
[58] G. Cvetič, F. Halzen, C. S. Kim, and S. Oh, Chin. Phys. C **41**, 113102 (2017).
[59] A. M. Sirunyan *et al.* (CMS Collaboration), Phys. Rev. Lett. **120**, 221801 (2018).